Supporting Information

Microbial degradation rates of natural bitumen

*Mark Pannekens[1], Lisa Voskuhl[1], Sadjad Mohammadian[1], Daniel Köster[2], Arne Meier[1], John. M. Köhne[3], Michelle Kulbatzki[1], Ali Akbari[1], Shirin Haque[4], Rainer U. Meckenstock[1]**

[1] Environmental Microbiology and Biotechnology, Aquatic Microbiology, University of Duisburg-Essen, 45141 Essen, Germany

[2] Instrumental Analytical Chemistry, University of Duisburg-Essen, 45141 Essen, Germany

[3] Department of Soil System Science, Helmholtz Centre for Environmental Research, 06120 Halle, Germany

[4] Department of Physics, Faculty of Science and Technology, The University of The West Indies, St. Augustine, Trinidad and Tobago

* Corresponding Author: Rainer U. Meckenstock, Environmental Microbiology and Biotechnology, Aquatic Microbiology, University of Duisburg-Essen, 45141 Essen, Germany, rainer.meckenstock@uni-due.de, Tel.: +49 (0201) 183 - 6601

Number of pages: 13

Number tables: 3

Number of figures: 1

List of content

Table S3: Stoichiometry for reactions for syntrophic hydrocarbon degradation of hydrocarbons present in petroleum reservoirs

Figure S1: Fluorescence images of drinking water biofilms grown on EPDM coupons and stained with Syto9 (green) and seven different lectins (red). Pictures were taken with a confocal laser scanning microscope. Excitation wavelengths were λ 488 nm, λ 561 nm, and λ 633 nm, respectively. Scale bars indicate 15 µm.

Experimental section and results

Geochemistry of water extracted from the bitumen body

For anion analysis, water samples extracted from bitumen were diluted with 1 M KOH (1:10) and centrifuged for 15 min at 16,000 x g. The supernatant was further diluted in deionized water (18.2 MΩ, TOC > 5ppb; Milli-Q®Advantage A10 device equipped with a Q-Gard®T2 filter, a Quantum®TEX filter, and a Millipak®Express 40 0.22 µm filter, Merck Millipore, Germany) 1:10 and 1:100, respectively. For cation analysis, water samples were diluted 1:10 with deionized water and centrifuged for 15 min at 16,000 x g. The supernatant was further diluted with deionized water 1:10. Cations were measured with a 850 professional ion chromatography system (Metrohm, Germany) equipped with a Metrosep C4 S-Guard/4.0 guard column and

Metrosep C4 250/4.0 analytical column. The eluent consisted of 1.7 mM nitric acid (Carl Roth, Germany) and 0.7 mM dipicolinic acid (Fluka™, UK). The flow rate was 0.9 ml min^{-1} at room temperature. The software Magic IC™ Net (Metrohm, Germany) version 2.3 was used for data analysis. Anions were measured with a Dionex DX 500 AS3500 ion chromatography system (Dionex, CA, USA) equipped with a ASRD Ultra II suppressor, a CD20 conductivity detector, a EG 50 gradient generator combined with an EluGen cartridge EGC II KOH, a AG17C 2x50 mm guard column and a AS17C 2x250 mm analytical column. A KOH gradient was applied starting with 10 mM for 1 min following a linear increase over 4.5 min to 50 mM. Afterwards, the concentrations declined over 1 min to 10 mM and remained constant for an additional minute before the next measurement. The flowrate was 0.38 ml min^{-1}. The software Chromeleon version 6.70 Build 1820 was used for data analysis. The results are shown in table S1.

Table S1. Measured ion concentrations (± standard deviation) in water extracted from Pitch Lake bitumen.

anion	concentration [mM]	cation	concentration [mM]
chloride	433.0 ± 27.0	sodium	218.4 ± 12.7
nitrite	0.0	ammonium	16.4 ± 0.6

sulfate	9.7 ± 3.9	potassium	5.5 ± 0.4
nitrate	0.0	calcium	1.1 ± 0.1
phosphate	31.7 ± 4.4	magnesium	1.2 ± 0.2

Droplet origin

A direct comparison of extracted water with seawater sampled from the coast nearby and surface water sampled from ponds on the Pitch Lake (presumably rainwater) showed strong differences in ion concentration and composition (results not shown), which agrees with Meckenstock et al., 2014, which compared the isotopic ratios of oxygen and hydrogen of extracted water with the local meteoric water line, indicating an origin from the deep subsurface.[1] Further, our 16S gene sequencing results show a consistently anaerobic community with nearly no aerobic surface contaminations (figure 2). These findings together strongly support a deep subsurface origin of our entrapped water droplets present in the Pitch Lake bitumen.

DNA extraction, 16S rRNA gene amplification, library preparation and sequencing

For DNA extraction of sessile cells, the remaining water was removed from the microcosms. The microcosms were opened and subsequently stored at -70 ˚C for 4 h. Scalpels were used to flake off thin pieces of the frozen bitumen surface. These pieces were collected with tweezers and transferred into bead-beating tubes containing 0.1 mm glass beads, ranging from 0.2 g to 0.7 g. Afterwards, 300 µl Miller phosphate buffer (Carl ROTH GmbH + Co. KG), 300 µl Miller SDS lysis buffer (Bernd Kraft GmbH, Thermo Fisher Scientific), and 600 µl phenol-chloroform-isoamyl alcohol solution [PCI, 25:24:1 (vol:vol:vol:), Thermo Fisher Scientific, USA] were added and gently mixed. Cell lysis was performed by bead-beating for 45 s at 5.5 m s^{-1}. Afterwards samples were centrifuged at 10.000 x g at 4 ˚C for 5 min. The aqueous supernatant was transferred to a phase lock gel heavy tube (Eppendorf, Germany), followed by the addition of an equal amount of chloroform-isoamyl alcohol solution [CI, 24:1 (vol:vol), Thermo Fisher Scientific, USA] and gentle mixing. Subsequently, the samples were centrifuged again at 10,000 x g at 4 ˚C for 5 min, and the supernatant of the upper layer was transferred into a new 2 ml reaction tubes. The samples were further proceeded by using the DNeasy PowerLyser Power Soil Kit (Qiagen GmbH, Germany) for DNA extraction according to the manufacturer's instructions. As the only deviation from the standard protocol, the amount of C4 buffer at step 12 was enhanced from 1200 to 1500 µl.[2-4]

For DNA extraction of planktonic cells, 1.5 ml liquid sample (time points 0 and 4) and 0.5 ml (time points 6 and 8) were used, respectively. The DNeasy PowerLyser Power Soil Kit (Qiagen GmbH, Germany) was used for DNA extraction according to the manufacturer's instructions. Modifications of the "Quick-Start Protocol" were made as follows: in step 3. samples were incubated for 5 min at 50 ˚C and 300 rpm in a thermoshaker, in step 4. samples were shaken for 45 s and 4000 rpm in a Precellys 24 tissue homogenizer (Bertin technologies SAS, France), in step 9. 500 µl supernatant was used instead of 600 µl, and in step 12. 650 µl supernatant was used instead of 750 µl.

After extraction, we used a modified purification protocol to remove remaining contaminations from the liquid sample extracts.[5-7] To this end, a solution containing 24.7 mM glycogen and 3 M sodium acetate was added (10 % v/v) to the DNA extract. Then, 400 µl of 99.5 % ethanol were added and incubated at 4 ˚C, overnight. Afterwards, samples were centrifuged at 15,000 x g for 30 min and the supernatant discarded. Thereafter, 200 µl 70 % ethanol were added and the tube was gently shaken. The samples were centrifuged again at 15,000 x g for 30 min and the supernatant was discarded. The samples were dried for 15 min at air and the extracted DNA was resuspended in 20 µl of C6 buffer solution of the extraction kit.

Former experiments (results not shown) showed an inhibition during the amplicon PCR of samples extracted from bitumen due to matrix effects. Therefore, a further cleaning procedure

modified from the Illumina protocol was applied before amplicon PCR. The samples were centrifuged at 7,500 x g for 3 min. Afterwards, the supernatants of each triplicate were pooled. Then, 60 µl of each sample were mixed with 50 µl MagSi-NGS Prep-Plus magnetic beads (Steinbrenner Laborsysteme GmbH, Mannheim, Germany) and incubated for 5 min. After the incubation, the samples were placed on a magnetic stand for 2 min and the supernatant was discarded. The samples remained on the magnetic stand and 200 µl of 80 % ethanol were added. After 30 s incubation, the ethanol was discarded followed by 5 min drying. Then, the magnetic stand was removed and 40 µl EB buffer were added and mixed 15x by pipette followed by a 2 min incubation. Afterwards, the samples were placed on a magnetic stand for 2 min, after which the supernatant was transferred into clean tubes for further analysis.

Amplification of the 16S rRNA genes, library preparation and sequencing were performed as described in Pannekens et al., 2020 with minor modifications: The 16S rRNA gene sequences were amplified by targeting the hypervariable V3-V4 region with forward primer S-D-Arch-0519-a-S-15 (5′-CAGCMGCCGCGGTAA-3′) and an overhang adaptor (5′-TCG TCG GCA GCG TCA GAT GTG TAT AAG AGA CAG CCT ACG GGN BGC ASC A-3′) and with reverse primer S-D-Bact-0785-b-A-18 (5′-GACTACHVGGGTATCTAATCC-3′) and an overhang adaptor (5′-GTC TCG TGG GCT CGG AGA TGT GTA TAA GAG ACA GGA CTA CNV GGG TAT CTA ATC C-3′).[8] The choice of primers and hypervariable region aimed at

covering the broadest possible spectrum of both bacteria and archaea.[9] The mothur version (version 1.44.0, last updated 19 March, 2019) was used for bioinformatic analysis. In addition, ambiguous bases shorter than 287 bp or longer than 289 bp were removed from the data set after merging forward and reverse reads. Version 138 of the SILVA database was used for alignment and the reads were rarified to the lowest detected read number of 8479 (sample 4_T0_1). Raw sequencing reads were deposited in the NCBI database under BioProject PRJNA645080.

Biofilm visualization on bitumen surface

The frozen bitumen surface (-70˚ C) was chipped off by scalpel and transferred with tweezers face up onto concaved object slides. Seven fluorescence labeled lectins with specific bounding to different polysaccharides were used for EPS visualization (table S2). A lectin solution was prepared containing Syto9 as DNA stain and 0.01 M 4-(2-hydroxyethyl)-1-piperazineethanesulfonic acid, 0.15 M NaCl, 0.1 mM $CaCl_2$ x $2H_2O$, 0.1 mM $MnCl_2$ x $4H_2O$, 0.1 mM $MgCl_2$ x $6H_2O$, 10 µM Sytgo9, 10 µg ml^{-1} of each lectin, and a pH of 7.5 (modified from manufacturers buffer solutions). The bitumen surface was covered with 50 µl of the lectin solution and incubated for 30 min in the dark. Afterwards, the lectin solution was removed with

a pipette and the bitumen surface was gently washed three times with deionized water.[10, 11] In addition, the staining solution was tested on drinking water biofilms grown on EPDM coupons (ethylene propylene diene monomer) according to Mackowiack (2019) (figure S1).[12] An epifluorescence microscope Eclipse Ni-E (Nikon; Japan) with FITC and DsRed filters, a CFI Plan Fluor 40x/0.75 or DLL Plan Fluor 20x/0.5 objective and the software Nis Elements version 5.11 was used for analysis of bitumen samples. A confocal laser scanning microscope and the LAS.X software version 3.7.2.22383 were used for drinking water biofilm samples according to Pannekens *et al.,* (2020).[8]

Table S2. List of used lectins, their shortcut, the specific binding and the excitation and emission wavelength of the associated fluorescent tags.

Name	Shortcut	Specific binding	Excitation in nm	Emission in nm
Concanavalin A	Con A	Mannose; Glucose; Alginate [11, 13, 14]	593	614
Peanut agglutinin	PNA	Galactose [13]	596	615
Ulex Europaeus Agglutinin I	UEA	Fucose [10, 11, 13]	652	672

Griffonia Simplicifolia Lectin II	GS II	N-acetylglucosamine [13]	596	615
Wheat germ agglutinin	WGA	N-acetylglucosamine [13, 14]	593	614
Soybean agglutinin	SBA	N-acetylgalactosamine; Galactose [13]	596	615
Oncorhynchus keta Lectin	CSL 3	Rhamnose [15]	554	568

Syto9-lectin tests on drinking water biofilms

To prove the staining potential and exclude the possibility of inhibiting or quenching effects due to lectin mixing, drinking water biofilms, grown for 14 days on an EPDM coupons, were stained as described above and examined with an epifluorescence microscope (figure S1).

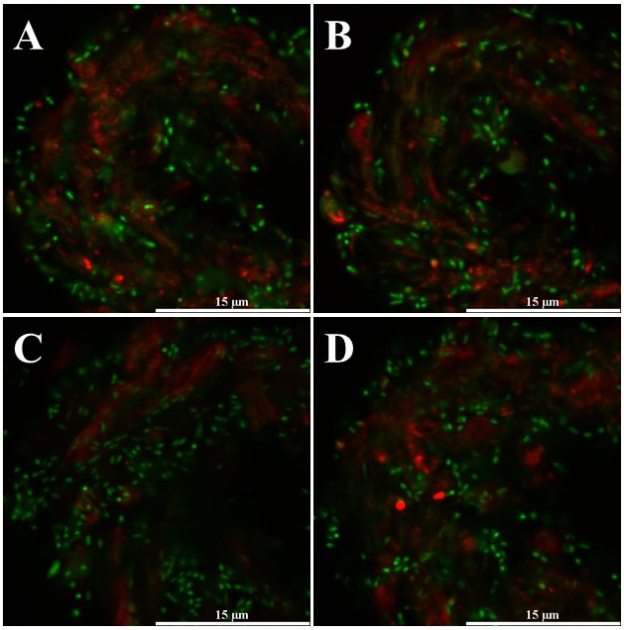

Figure S1. Fluorescence images of drinking water biofilms grown on EPDM coupons and stained with Syto9 (green) and seven different lectins (red). Pictures were taken with a confocal laser scanning microscope. Excitation wavelengths were λ 488 nm, λ 561 nm, and λ 633 nm, respectively. Scale bars indicate 15 µm.

The images clearly show green fluorescent microbial cells embedded in a red fluorescent EPS matrix. No inhibition effects were observable.

Sulfate measurements during the experiment

Liquid sample were centrifuged for 10 min at 16,000 x g, the supernatant was diluted 1:10 with 0.1 M KOH and centrifuged again for 10 min at 16,000 x g. The supernatant was then diluted 1:50 or 1:100 with deionized water (18.2 MΩ, TOC > 5ppb), respectively. Sulfate was measured by a Dionex Aquion ion chromatography system (Thermo Scientific, USA) equipped with a Dionex IonPac™ AG23-4 µm 2x50 mm guard column, a Dionex IonPac™ AG23-4 µm 2x250 mm analytical column, an AERS 500 Carbonate 2 mm suppressor, and a DS6 heated conductivity cell detector. A carbonate buffer (0.0008 M $NaHCO_3$; 0.0045 M Na_2CO_3) served as eluent, with a flow rate of 0.25 ml min^{-1} at 30 ˚C. The software Chromeleon (Thermo Scientific, MA, USA) version 7.2 SR5 was used for data analysis.

3D imaging of bitumen – droplet distribution

The water droplet distribution in the bitumen was determined via computed tomography scanning. Liquid oil seeping to the surface at different locations on the Pitch Lake was either filled directly on site (3 columns) or in the laboratory (3 columns) into round plastic columns (15 cm in length with a diameter of 1.5 cm or 1 cm, respectively). The top and bottom were sealed with rubber stoppers in the field and exchanged with hot glue in the laboratory. The sealed columns were placed on plastic stands and stored at 4 ˚C until analysis, where the heavy

oil remained solid. The samples were scanned with X-ray tomography (X-tek XT H 225, Nikon Metrology, Japan) at an energy of 90 kV and a beam current of 155 μA. In total, 2000 projections were taken with 2 frames per projection and an exposure time of 1 s. The projections were then reconstructed into a 3D image using the software X-tec CT Pro 3D. The final images had 8-bit grey scale resolutions and 12.5 μm spatial resolution. The quantitative image analysis was carried out using the Fiji software (version 1.52i).[16] A rectangular inner sub volume with a size of 880 x 880 x 1000 voxels was analyzed for each image (total volume ~1.5 ml). The raw images were filtered using a 3D median filter with a radius of 3 voxels and the image contrast was then improved using CLAHE routine in Fiji. Segmentation into water and oil phases were carried out with a hysteresis segmentation method after Vogel and Kretzschmar (1996).[17] The lower and upper threshold levels were selected individually for each image. Another median filter with a radius of 3 voxels was applied to the segmented images to remove small objects. Quantification of water droplet properties was carried out using 3D LibMorphJ plugin.[18] The water droplets in each 3D image were labelled and their size and surface area were quantified. The frequency of each droplet size was then calculated by counting voxels in each object. A total of 7 scans were used.

Bitumen mineralization to carbon dioxide

The stepwise degradation of crude oil or bitumen by fermenting and sulfate reducing bacteria, leads to a variety of different intermediates like short-chain fatty acids, alcohols, acetate, formate, and hydrogen. The final mineralization product is carbon dioxide (table S3).[19-25] This makes carbon dioxide a good reference product for biodegradation under sulfate reducing conditions.

Table S3 Reaction stoichiometries for syntrophic hydrocarbon degradation in petroleum reservoirs.

Substrate	Stoichiometric equation	
Syntrophic hydrocarbon oxidation		
Toluene	$C_7H_8 + 7H_2O \rightarrow 3.5CH_3COO^- + 4H_2 + 3.5H^+$	19
Naphthalene	$C_{10}H_8 + 10H_2O \rightarrow 5CH_3COO^- + 4H_2 + 5H^+$	19
Hexadecane	$C_{16}H_{34} + 16H_2O \rightarrow 8CH_3COO^- + 17H_2 + 8H^+$	19, 26, 27
Syntrophic acetate oxidation		
Acetate	$CH_3COO^- H^+ 2H_2O \rightarrow 2CO_2 + 4H_2$	27, 28
Hydrocarbon degradation by sulfate reduction		
Acetate	$CH_3COO^- + SO_4^{2-} \rightarrow 2HCO_3^- + HS^-$	
Benzene	$C_6H_6 + 3H_2O + 3.75SO_4^{2-} \rightarrow 6HCO_3^- + 3.75HS^- + 2.25H^+$	21
Toluene	$C_7H_8 + 4.5SO_4^{2-} + 3H_2O \rightarrow 7HCO_3^- + 2.5H^+ + 4.5HS^-$	24
Decane	$C_{10}H_{22} + 7.75SO_4^{2-} + 5.5H^+ \rightarrow 10HCO_3^- + 7.75H_2S + H_2O$	25
Naphthalene	$C_{10}H_8 + 6SO_4^{2-} + 6H_2O \rightarrow 10HCO_3^- + 6HS^- + 4H^+$	21
2-methylnaphthalene	$C_{11}H_{10} + 6.75SO_4^{2-} + 6H_2O \rightarrow 11HCO_3^- + 6.75HS^- + 4.25H^+$	21
Phenanthrene	$C_{14}H_{10} + 8.25SO_4^{2-} + 9H_2O \rightarrow 14HCO_3^- + 8.25HS^- + 5.75H^+$	21
Hexadecane	$C_{16}H_{34} + 12.25SO_4^{2-} + 8.5H^+ \rightarrow 16HCO_3^- + 12.25H_2S + H_2O$	22, 23

REFERENCES

1. Meckenstock, R. U.; von Netzer, F.; Stumpp, C.; Lueders, T.; Himmelberg, A. M.; Hertkorn, N.; Schmitt-Kopplin, P.; Harir, M.; Hosein, R.; Haque, S., Water droplets in oil are microhabitats for microbial life. *Science* **2014,** *345*, 673-676.

2. Himmelberg, A. Life in pitch-Bacteria in a natural oil emitting lake help to understand anaerobic biodegradation of polycyclic aromatic hydrocarbons. PhD-Thesis, Technical University of Munich, **2019**.

3. Lueders, T.; Manefield, M.; Friedrich, M. W., Enhanced sensitivity of DNA-and rRNA-based stable isotope probing by fractionation and quantitative analysis of isopycnic centrifugation gradients. *Environ Microbiol* **2004,** *6*, 73-78.

4. Gabor, E. M.; de Vries, E. J.; Janssen, D. B., Efficient recovery of environmental DNA for expression cloning by indirect extraction methods. *FEMS Microbiol Ecol* **2003,** *44*, 153-163.

5. Zeugin, J. A.; Hartley, J. L., Ethanol precipitation of DNA. *Focus* **1985,** *7*, 1-2.

6. Crouse, J.; Amorese, D., Ethanol precipitation: ammonium acetate as an alternative to sodium acetate. *Focus* **1987,** *9*, 3-5.

7. Sambrook, H., Molecular cloning: a laboratory manual. Cold Spring Harbor, NY. **1989**.

8. Pannekens, M.; Voskuhl, L.; Meier, A.; Müller, H.; Haque, S.; Frösler, J.; Brauer, V.; Meckenstock, R., Densely populated water droplets in heavy oil seeps. *Appl Environ Microbiol* **2020,** *86*, 1-12.

9. Klindworth, A.; Pruesse, E.; Schweer, T.; Peplies, J.; Quast, C.; Horn, M.; Glöckner, F. O., Evaluation of general 16S ribosomal RNA gene PCR primers for classical and next-generation sequencing-based diversity studies. *Nucleic Acids Res* **2013,** *41*, e1-e1.

10. Neu, T. R.; Swerhone, G. D.; Lawrence, J. R., Assessment of lectin-binding analysis for in situ detection of glycoconjugates in biofilm systems. *Microbiology* **2001,** *147*, 299-313.

11. Peltola, M.; Neu, T. R.; Raulio, M.; Kolari, M.; Salkinoja-Salonen, M. S., Architecture of Deinococcus geothermalis biofilms on glass and steel: a lectin study. *Environ Microbiol* **2008,** *10*, 1752-1759.

12. Mackowiak, M. Interaction of Enteric Viruses with Aquatic Biofilms in the Urban Water Cycle. PhD-thesis, University of Duisburg-Essen, **2019**.

13. Thyssen, C. Biofilm formation by the manganese-oxidizing bacterium *Leptothrix discophora strain SS-1* and corrosion of stainless steel. PhD-thesis, University of Duisburg-Essen, **2018**.

14. Strathmann, M.; Wingender, J.; Flemming, H.-C., Application of fluorescently labelled lectins for the visualization and biochemical characterization of polysaccharides in biofilms of *Pseudomonas aeruginosa*. *J Microbiol Methods* **2002,** *50*, 237-248.

15. Shiina, N.; Tateno, H.; Ogawa, T.; Muramoto, K.; Saneyoshi, M.; Kamiya, H., Isolation and characterization of L-rhamnose-binding lectins from chum salmon (Oncorhynchus keta) eggs. *Fish Sci* **2002,** *68*, 1352-1366.

16. Schindelin, J., Fiji: An open-source platform for biological-image analysis. *In Nat Methods*, **2019**; Vol. 9, pp 676–682.

17. Vogel, H.; Kretzschmar, A., Topological characterization of pore space in soil—sample preparation and digital image-processing. *Geoderma* **1996,** *73*, 23-38.

18. Legland, D.; Arganda-Carreras, I.; Andrey, P., MorphoLibJ: integrated library and plugins for mathematical morphology with ImageJ. *Bioinformatics* **2016,** *32*, 3532-3534.

19. Gieg, L. M.; Fowler, S. J.; Berdugo-Clavijo, C., Syntrophic biodegradation of hydrocarbon contaminants. *Curr Opin Biotechnol* **2014,** *27*, 21-29.

20. Jiménez, N.; Richnow, H. H.; Vogt, C.; Treude, T.; Krüger, M., Methanogenic hydrocarbon degradation: evidence from field and laboratory studies. *J Mol Microbiol Biotechnol* **2016,** *26*, 227-242.

21. Meckenstock, R. U.; Boll, M.; Mouttaki, H.; Koelschbach, J. S.; Tarouco, P. C.; Weyrauch, P.; Dong, X.; Himmelberg, A. M., Anaerobic degradation of benzene and polycyclic aromatic hydrocarbons. *J Mol Microbiol Biotechnol* **2016,** *26*, 92-118.

22. Mbadinga, S. M.; Wang, L.-Y.; Zhou, L.; Liu, J.-F.; Gu, J.-D.; Mu, B.-Z., Microbial communities involved in anaerobic degradation of alkanes. *Int Biodeter Biodegr* **2011,** *65*, 1-13.

23. Aeckersberg, F.; Bak, F.; Widdel, F., Anaerobic oxidation of saturated hydrocarbons to CO_2 by a new type of sulfate-reducing bacterium. *Arch Microbiol* **1991,** *156*, 5-14.

24. Heider, J.; Spormann, A. M.; Beller, H. R.; Widdel, F., Anaerobic bacterial metabolism of hydrocarbons. *FEMS Microbiol Rev* **1998,** *22*, 459-473.

25. Rueter, P.; Rabus, R.; Wilkest, H.; Aeckersberg, F.; Rainey, F. A.; Jannasch, H. W.; Widdel, F., Anaerobic oxidation of hydrocarbons in crude oil by new types of sulphate-reducing bacteria. *Nature* **1994,** *372*, 455-458.

26. Head, I.; Larter, S.; Gray, N.; Sherry, A.; Adams, J.; Aitken, C.; Jones, D.; Rowan, A.; Huang, H.; Röling, W., Hydrocarbon degradation in petroleum reservoirs. In *Handbook of hydrocarbon and lipid microbiology*, Springer: **2010;** pp 3097-3109.

27. Jones, D.; Head, I.; Gray, N.; Adams, J.; Rowan, A.; Aitken, C.; Bennett, B.; Huang, H.; Brown, A.; Bowler, B., Crude-oil biodegradation via methanogenesis in subsurface petroleum reservoirs. *Nature* **2008,** *451*, 176-180.

28. Xu, D.; Zhang, K.; Li, B.-G.; Mbadinga, S. M.; Zhou, L.; Liu, J.-F.; Yang, S.-Z.; Gu, J.-D.; Mu, B.-Z., Simulation of in situ oil reservoir conditions in a laboratory bioreactor testing

for methanogenic conversion of crude oil and analysis of the microbial community. *Int Biodeterior Biodegradation* 2019, *136*, 24-33.